Journal of Superconductivity and Novel Magnetism (2018) 31:3175–3182
https://doi.org/10.1007/s10948-018-4599-6

ORIGINAL PAPER

The Effect of Inhomogeneous Phase on the Critical Temperature of Smart Meta-superconductor MgB_2

Honggang Chen[1] · Yongbo Li[1] · Guowei Chen[1] · Longxuan Xu[1] · Xiaopeng Zhao[1]

Received: 29 January 2018 / Accepted: 5 February 2018 / Published online: 21 February 2018

Abstract
The critical temperature (T_C) of MgB_2, one of the key factors limiting its application, is highly desired to be improved. On the basis of the meta-material structure, we prepared a smart meta-superconductor structure consisting of MgB_2 micro-particles and inhomogeneous phases by an ex situ process. The effect of inhomogeneous phase on the T_C of smart meta-superconductor MgB_2 was investigated. Results showed that the onset temperature (T_C^{on}) of doping samples was lower than those of pure MgB_2. However, the offset temperature (T_C^{off}) of the sample doped with Y_2O_3:Eu^{3+} nanosheets with a thickness of 2 $\sim$ 3 nm which is much less than the coherence length of MgB_2 is 1.2 K higher than that of pure MgB_2. The effect of the applied electric field on the T_C of the sample was also studied. Results indicated that with the increase of current, T_C^{on} is slightly increased in the samples doping with different inhomogeneous phases. With increasing current, the T_C^{off} of the samples doped with nonluminous inhomogeneous phases was decreased. However, the T_C^{off} of the luminescent inhomogeneous phase doping samples increased and then decreased with increasing current.

Keywords Smart meta-superconductor MgB_2 · Y_2O_3:Eu^{3+} nanosheets · Inhomogeneous phase · Applied electric field·T_C

1 Introduction

Since Akimitsu et al. [1] discovered the binary compound MgB_2 superconductor in 2001, this material has attracted considerable attention because of its simple structure, low cost, large coherence length, and relatively high transition temperature (T_C = 39 K) [2]. Improving the superconducting transition temperature of MgB_2 can not only increase its application but also promote the development of superconductivity theory. The most commonly used method in improving the critical temperature (T_C) of MgB_2 is chemical doping. Substituting Mg and B with Al and C, respectively, in MgB_2 forms the displacement doping. However, results showed that the two kinds of doping reduce the T_C of MgB_2 [3–7]. In addition, another possible method for improving the T_C is increasing the density of holes by partially substituting Mg with Li. Nevertheless, experimental results showed that T_C is still reduced [8, 9]. The T_C of MgB_2 is reduced because of the presence of the dopant as an impurity in MgB_2, which results in poor grain connectivity and doping into other substances to distort the MgB_2 lattice. Although it is important to increase the T_C of MgB_2 beyond the theoretical value, it also presents considerable challenge and requires further investigation.

Meta-material, a type of artificially structured composite material, is composed of the matrix material and its unit material. The properties of these materials mainly depend on the artificial structure, which can realize many special functions [10–15]. With the development of meta-material, the use of meta-material concept to design superconducting materials to improve its T_C has been recognized. We proposed the introduction of electroluminescence (EL) materials in meta-materials to enhance the superconducting transition temperature through EL [16, 17]. Zhang et al. [18] used an in situ solid-phase sintering process to dope Y_2O_3:Eu^{3+} EL materials in MgB_2; their results showed that the T_C of MgB_2 can be enhanced by doping of Y_2O_3:Eu^{3+} EL materials. However, in the in situ sintering process, the raw material B reacts with the Y_2O_3:Eu^{3+} EL material to form the impurity phase of YB_4. To avoid the formation of the impurity phase of YB_4, Tao et al. [19] doped Y_2O_3:Eu^{3+}

✉ Xiaopeng Zhao
xpzhao@nwpu.edu.cn

[1] Smart Materials Laboratory, Department of Applied Physics, Northwestern Polytechnical University, Xi'an 710129, People's Republic of China

EL material into MgB_2 by an ex situ solid-phase sintering process. Experimental results indicated that the Y_2O_3:Eu^{3+} EL material doping can improve the superconducting transition temperature of MgB_2; moreover, the morphology and size of the Y_2O_3:Eu^{3+} EL material affect the T_C of MgB_2. To improve the distribution and connectivity of the inhomogeneous-phase dopants, the effect of different concentrations and sizes of YVO_4:Eu^{3+} microsheets EL material on the superconducting transition temperature of MgB_2 was studied. Results showed that the T_C^{off} of doped samples increases by 1.6 K compared with that of pure MgB_2 when the doping concentration is 2.0 wt%. Recently, Smolyaninov et al. [20–24] proposed that material can be designed as a meta-material structure with an effective dielectric constant $\varepsilon_{eff} \approx 0$, which can improve the T_C of the material. They also confirmed the material performance in their experiment.

For superconducting samples, the magnitude of the test current directly affects the accuracy of the test results. Considerably low current tends to decrease the useful voltage signal of the sample. Hence, the requirement of the voltage drop measurement instrument is high. When the current is significantly large, although the requirement of the voltage drop measurement instrument can be reduced, it will increase the thermal effect of the sample. Consequently, a large temperature hysteresis occurs, which affects the acquisition of real data [25, 26]. Ye et al. [27, 28] found that superconducting transition in unconventional superconductors ZrNCl and MoS_2 through carrier doping was induced by an applied electric field. Changing the applied electric field can obtain different transition temperatures; ZrNCl and MoS_2 display a transition temperature (T_C) of 15.2 and 10.8 K, respectively, on the optimum carrier doping.

On the basis of the idea of meta-material structure, our group proposed a smart meta-superconductor with a sandwich structure, where MgB_2 particles are used as the matrix material; the EL material distributed around the MgB_2 particles are as inhomogeneous phase. When evaluating the curve of the temperature dependence of resistivity (R–T) of the samples, it was found that in the local electric field, MgB_2 particles act as microelectrodes, which promote the EL of inhomogeneous phase EL materials, and that the inhomogeneous phase significantly improves the T_C [18, 19]. In this paper, the responses of the critical temperature of MgB_2 to inhomogeneous phase doping and changing the applied electric field are systematically studied. At first, we prepared the Y_2O_3:Eu^{3+}, Y_2O_3, and Y_2O_3:Sm^{3+} nanosheet inhomogeneous phases; they were doped into MgB_2 by an ex situ process. The effects of doping Y_2O_3:Sm^{3+}/Y_2O_3 nonluminous inhomogeneous phase or Y_2O_3:Eu^{3+} EL inhomogeneous phase on the superconducting properties of MgB_2 were investigated. Then, on the basis of the theory that the material with a meta-structure and an effective dielectric constant close to zero can improve the T_C of the material, Y_2O_3:Eu^{3+} microsheets and nano-Ag solution were doped into MgB_2 to change the dielectric constant of the system; the superconducting properties of doping samples were also evaluated. Finally, we further examined the influence of the applied electric field on the EL and nonluminous inhomogeneous phase doping samples.

2 Experiment

2.1 Preparation of Nanosheets/Microsheets

At first, a certain amount of Y_2O_3 and Eu_2O_3 powder were added to 4 mL of concentrated nitric acid under stirring and heating at 70 °C for 1 h to obtain the $Y(Eu)(NO_3)_3$ white crystals. Afterward, some of the white crystals were dissolved in 24 mL of benzyl alcohol with constant stirring, and 6 mL of octylamine was added in the above solution and stirred for 30 min. Finally, the resulting solution was transferred to a reaction still heated at 160 °C for 24 h. The obtained precipitates were separated via centrifugation, washed several times with ethanol, and then dried in air at 60 °C for 12 h. The final products (Y_2O_3:Eu^{3+} nanosheets, marked as N1) were prepared by calcination at 800 °C for 2 h. Moreover, Y_2O_3 nanosheets (marked as N2) and Y_2O_3:Sm^{3+} nanosheets (marked as N3) were obtained by changing the raw material from the above-mentioned procedures [29], whereas YVO_4:Eu^{3+} microsheets (marked as N4) and Y_2O_3:Eu^{3+} microsheets (marked as N5) [30] were obtained by changing both the raw materials and the experimental conditions.

2.2 Preparation of Doped MgB_2-Based Superconductors

The concentration of nano-Ag solution in the experiment was 2000 ppm. The particle size was 15 nm, and the solvent was anhydrous ethanol.

MgB_2 powder and nanosheet/microsheet dopants (MgB_2 powder, microsheet dopant, and nano-Ag solution) were mixed in 15 mL of ethanol to form a suspension. The suspension was transferred into a culture dish after 30 min of sonication. Subsequently, the dish was placed in a vacuum oven for 4 h at 60 °C. The resultant black powder was pressed into tablets. Finally, the tablets were placed in tantalum vessels and annealed at 800 °C for 2 h at heating and cooling rates were of 10 and 5 °C min^{-1}, respectively. Afterward, the final products were obtained. For convenience of description, symbols were used to represent the samples. Furthermore, a pure MgB_2 sample marked as A was prepared for comparison. The symbols, dopant

Table 1 Symbols, dopant types, and dopant concentrations of each sample

Symbols of samples	A	B	C	D	E	F	G	H
Dopant types	None	N2	N3	N1	N4	N5	N5	N5
Dopant concentrations (wt%)	0	2	2	2	2	2	2	2
Nano-Ag concentrations (wt%)	0	0	0	0	0	0	0.2	0.4

types, and dopant concentrations of each sample are shown in Table 1.

3 Results and Discussion

Figure 1a–c shows the SEM images of YVO_4:Eu^{3+} microsheets and Y_2O_3:Eu^{3+} microsheets, and the TEM image of Y_2O_3:Eu^{3+} nanosheets, respectively. Figure 1d shows the AFM image of the Y_2O_3:Eu^{3+} nanosheets. Figure 1e presents the thickness of Y_2O_3:Eu^{3+} nanosheets. We know the prepared of YVO_4:Eu^{3+} and Y_2O_3:Eu^{3+} sheets show varying sizes. The sizes of YVO_4:Eu^{3+} and Y_2O_3:Eu^{3+} microsheets are 1–2 and 0.5–1 μm, respectively, and the size of Y_2O_3:Eu^{3+} nanosheets is approximately 50 nm. The thickness of the Y_2O_3:Eu^{3+} nanosheets is about 2 $\sim$ 3 nm, which is much less than the coherence length of MgB_2.

Figure 2 shows the X-ray diffraction (XRD) patterns of the partial samples and the SEM image of pure MgB_2. XRD results showed that the main phase is MgB_2. A small number of MgO and Mg impurities are also observed, which may broaden the superconducting transition temperature. MgO, which was formed during the preparation of MgB_2,

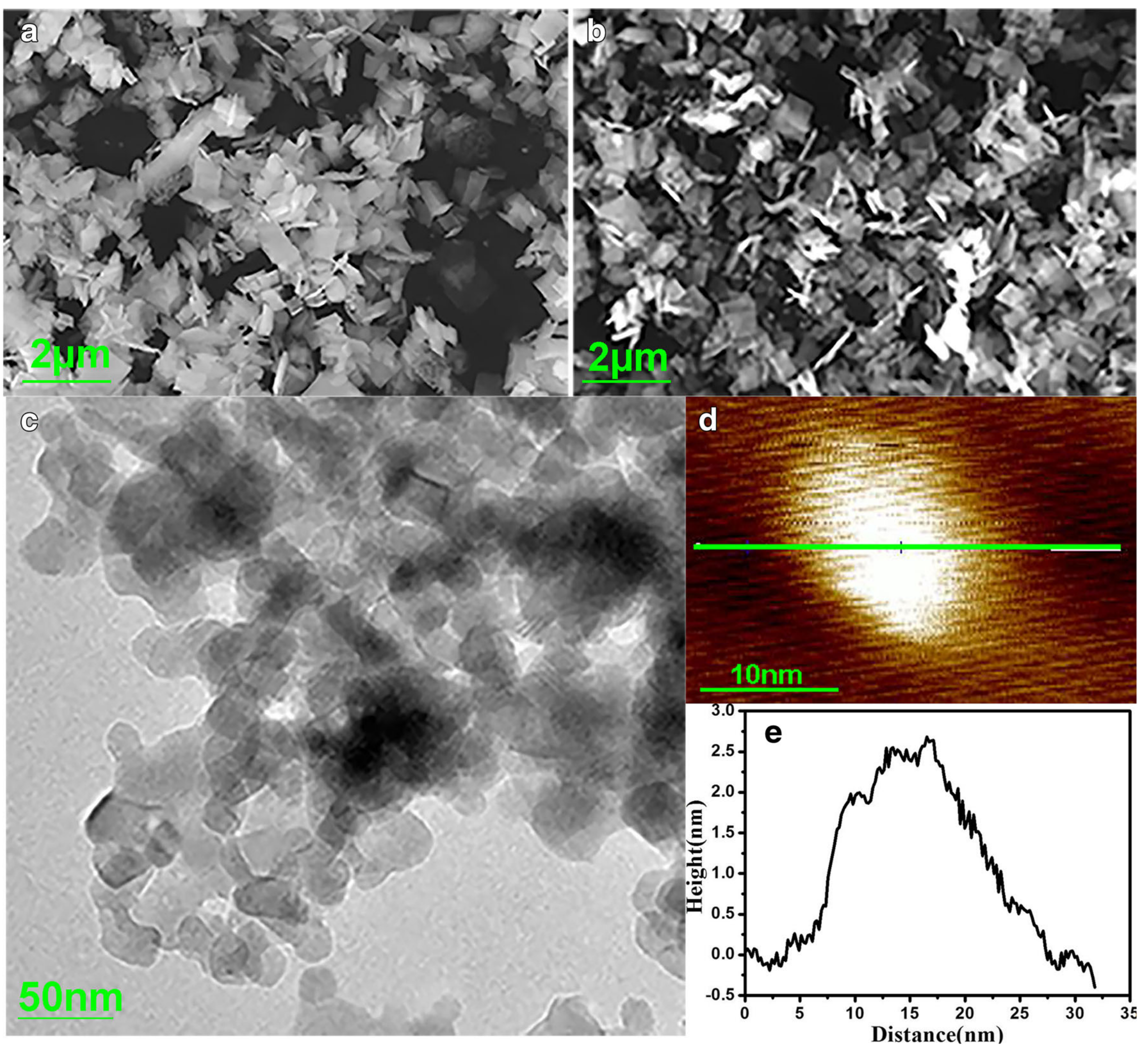

Fig. 1 SEM images of **a** YVO_4:Eu^{3+} microsheets (N4), **b** Y_2O_3:Eu^{3+} microsheets (N5), and **c** TEM image of Y_2O_3:Eu^{3+} nanosheets (N1); **d** AFM image of the Y_2O_3:Eu^{3+} nanosheets. **e** Height profile corresponding to the lines draw in **d**

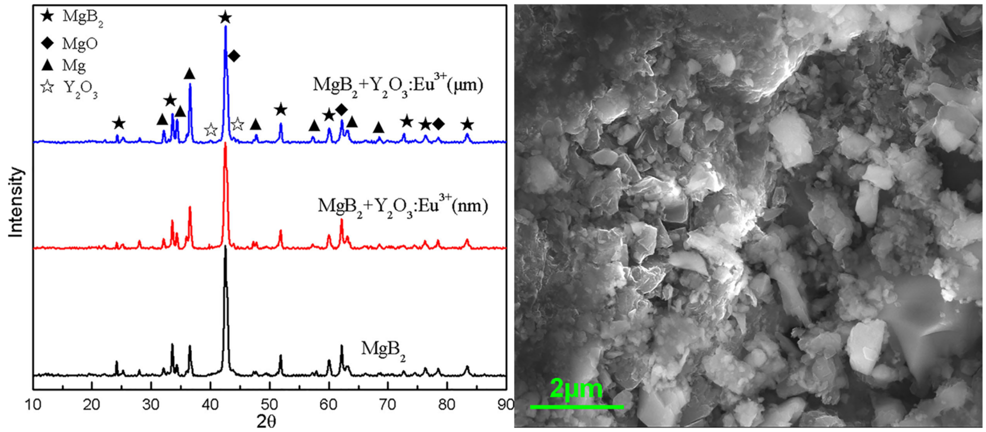

Fig. 2 X-ray diffraction patterns of MgB_2, $MgB_2 + 2$ wt% $Y_2O_3:Eu^{3+}$ (nm), $MgB_2 + 2$ wt% $Y_2O_3:Eu^{3+}$ (μm), and SEM image of pure MgB_2

is present in all samples. We also observed the existence of the Y_2O_3 in the doping samples. The SEM image shows that the irregularly shaped MgB_2 particles are mainly about 0.2–2 μm in size. The boundary between particles is also evident, which also broadens the superconducting transition temperature.

The XRD pattern of MgB_2 doped with $Y_2O_3:Eu^{3+}$ nanosheets is shown in Fig. 2. Because of the low content of $Y_2O_3:Eu^{3+}$ nanosheets, the Y_2O_3 peak is not obvious in the XRD pattern. To further prove that the sample is adulterated with $Y_2O_3:Eu^{3+}$ nanosheets, we performed an elemental analysis of the sample, and results are shown in Fig. 3. Figure 3a presents the SEM image of MgB_2 doped with $Y_2O_3:Eu^{3+}$ nanosheets. Figure 3b–d illustrates the distribution of certain chemical elements; the corresponding element is listed at the top right corner of each figure. According to the element distribution map, the sample contains a large number of Mg, and $Y_2O_3:Eu^{3+}$ nanosheet inhomogeneous phase dopants distributed around the MgB_2 particles.

Figure 4 depicts the R–T curve of the pure MgB_2 and MgB_2 doped with $Y_2O_3:Eu^{3+}$, Y_2O_3, and $Y_2O_3:Sm^{3+}$ nanosheets. The two characteristic temperatures, namely T_C^{on} and T_C^{off}, on each R–T curve are discussed. (1) The black curve shows the R–T curve of pure MgB_2 (A). The T_C^{on} and T_C^{off} of pure MgB_2 are 38.2 K and 33.6 K, respectively, the range of superconducting transition temperature is broad, this phenomenon is largely attributed to that the samples contain MgO and Mg impurities and exhibit poor grain connectivity [31]. (2) The resistivity of MgB_2 doped with

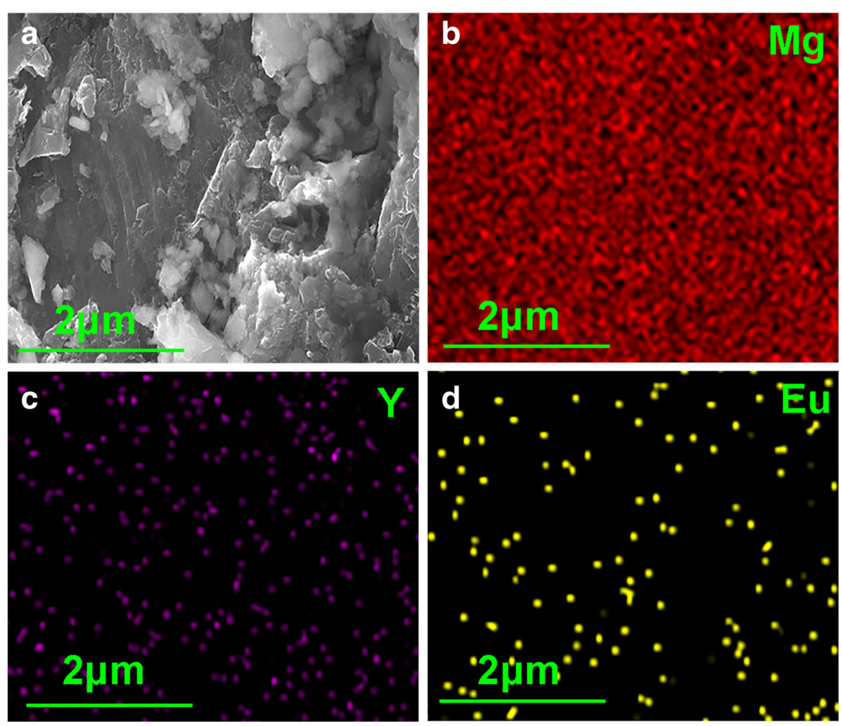

Fig. 3 SEM image of **a** $MgB_2 + 2$ wt% $Y_2O_3:Eu^{3+}$ (nm) (D) and chemical element distribution map (**b**–**d**)

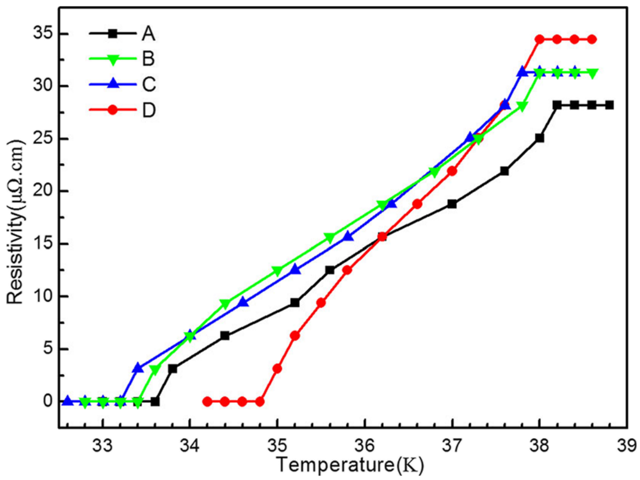

Fig. 4 Temperature-dependent resistivity of MgB_2 doped with different nano-sheets (pure MgB_2 (A), MgB_2+2 wt% Y_2O_3 (nm) (B), MgB_2 + 2 wt% Y_2O_3:Sm^{3+} (nm) (C), MgB_2 + 2 wt% Y_2O_3:Eu^{3+} (nm) (D))

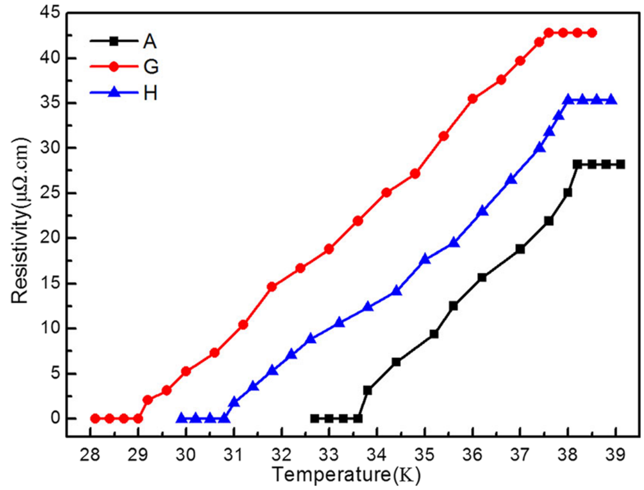

Fig. 5 Temperature-dependent resistivity of MgB_2 doped with Y_2O_3:Eu^{3+} microsheets and nano-Ag solution (MgB_2 (A), MgB_2 + 2 wt% Y_2O_3:Eu^{3+} (μm) + 0.2 wt% Ag (G), MgB_2+2 wt% Y_2O_3:Eu^{3+} (μm) + 0.4 wt% Ag (H)

nanosheets is higher than that of pure MgB_2. (3) The T_C^{off} of MgB_2 doped with Y_2O_3:Eu^{3+} nanosheets increases by 1.2 K compared with that of pure MgB_2, which may be due to the Y_2O_3:Eu^{3+} nanosheets EL material distributed around the MgB_2 particles to form a special response meta-structure. Y_2O_3:Eu^{3+} nanosheets would generate an EL during the measurement of *R*–*T* curve of the sample, which may improve the superconducting transition temperature [19]. (4) The T_C^{off} of MgB_2 doped with Y_2O_3 and Y_2O_3:Sm^{3+} nanosheets are lower than that of the pure MgB_2 sample. The MgB_2 doped with Y_2O_3:Sm^{3+} nanosheets presents the lowest T_C^{off}. The T_C^{on} of all of the MgB_2 doped with nanosheets is lower than that of the pure MgB_2. The T_C^{on} values of MgB_2 doped with Y_2O_3 and Y_2O_3:Eu^{3+} nanosheets are reduced by 0.2 K, and MgB_2 doped with Y_2O_3:Sm^{3+} nanosheets is reduced by 0.4 K.

Smolyaninov et al. proposed that MgB_2 doped with 5-nm diamond particles can make the dielectric constant close to 0; consequently, the superconducting transition temperature of the MgB_2-based metamaterial superconductor can reach the liquid nitrogen temperature [32]. On the basis of the idea that changing the effective dielectric constant can increase the superconducting transition temperature of a meta-superconductor, we prepared MgB_2 doped with Y_2O_3:Eu^{3+} microsheets and nano-Ag solution to change the dielectric constant of the system so as to improve the superconducting transition temperature of MgB_2. Figure 5 presents the *R*–*T* curve of the MgB_2 doped with Y_2O_3:Eu^{3+} microsheets and nano-Ag solution. However, this graph indicated that the MgB_2 doped with Y_2O_3:Eu^{3+} microsheets and nano-Ag solution fails to improve the T_C of MgB_2. All of the doped samples exhibit superconducting transition. The resistivity in the normal state increases, and the superconducting transition temperature of MgB_2 doped with nano-Ag solution decreases remarkably.

Figure 6 presents the *R*–*T* curves of six different doped samples under different currents, the upper left and bottom right corners are enlarged graphs of corresponding T_C^{on} and T_C^{off}, respectively. Table 2 provides a list of the concrete values of T_C^{on} and T_C^{off}. Figure 7 shows the relationship between the T_C^{off} of doped samples and currents. According to the results presented in Figs. 6, 7, and Table 2, the following trends are determined: (1) With increasing current, the T_C^{off} values of pure MgB_2 (A) and MgB_2 doped with Y_2O_3 nanosheets (B) and Y_2O_3:Sm^{3+} nanosheets (C) decrease, and the T_C^{on} and T_C^{off} of MgB_2 doped with Y_2O_3 nanosheets and Y_2O_3:Sm^{3+} nanosheets are lower than those of pure MgB_2 at the corresponding current; this result is attributed to impurity doping. (2) The T_C^{off} of MgB_2 doped with Y_2O_3:Eu^{3+} micro-sheets (F), Y_2O_3:Eu^{3+} nanosheets (D), and YVO_4:Eu^{3+} micro-sheets (E) show a slight increase at a current less than or equal to 100 mA. However, when the current is larger than 100 mA, T_C^{off} decreases with the increasing current. This result may be due to the considerably high current, which results in a remarkable thermal effect. Consequently, the temperature gradient in the superconducting sample is increased, thereby increasing the influence of thermoelectric potential on the measurements [25]. (3) The T_C^{on} of the pure MgB_2 sample remains unchanged when increasing current, whereas that of the doped samples show a slight increase. The T_C^{on} values of all nonluminous inhomogeneous phase doping samples are no more than 38.2 K, but those of samples doped with EL inhomogeneous phases are more than 38.2 K at a certain current. Japanese scientists observed superconducting transition by changing the electric field in

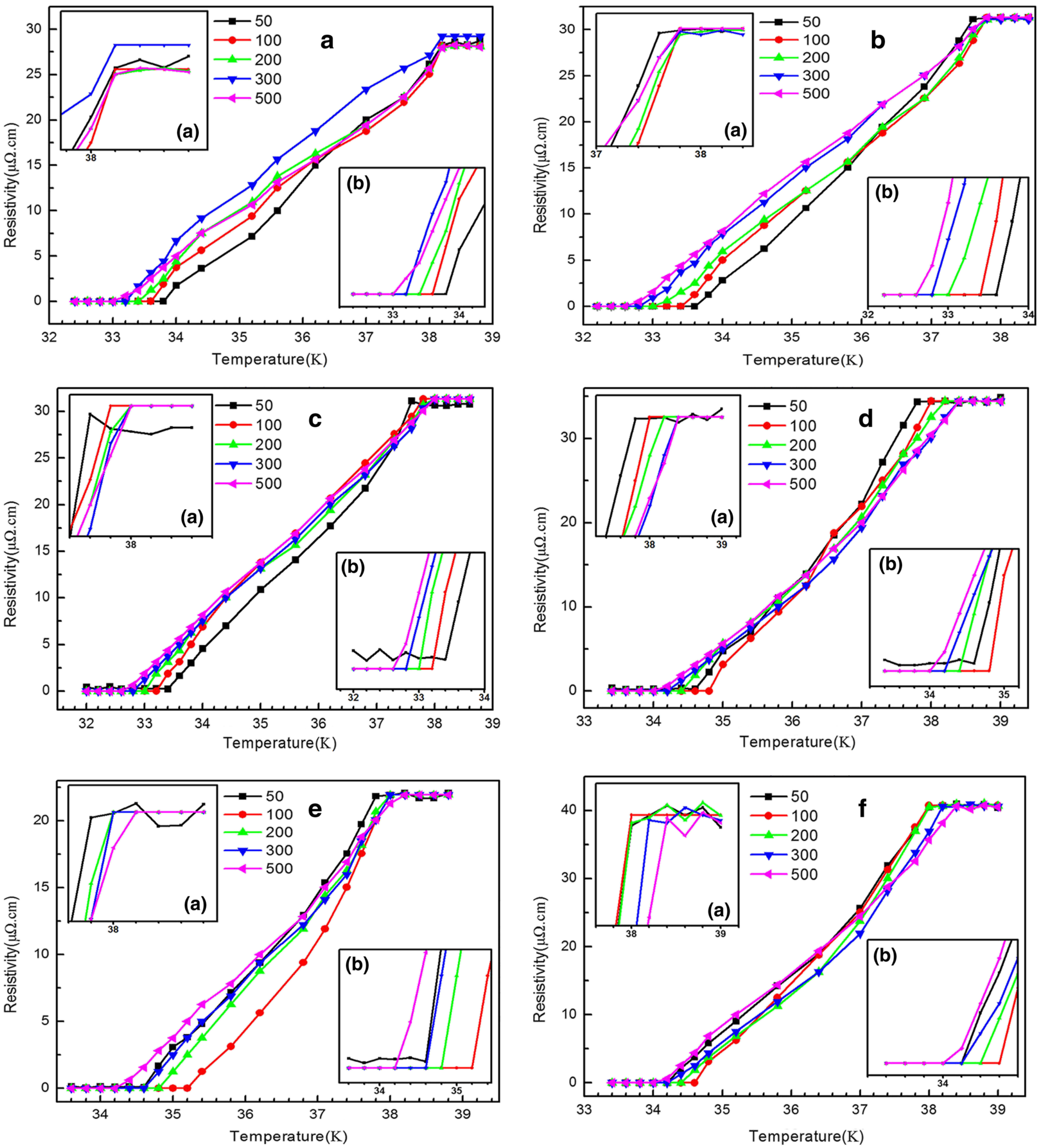

Fig. 6 Temperature-dependent resistivity of doped samples under different currents (50, 100, 200, 300, 500 mA)

Table 2 The T_C^{off} and T_C^{on} of doped samples under different currents

	A/K	B/K	C/K	D/K	E/K	F/K
50 mA	33.8–38.2	33.6–37.6	33.4–37.6	34.6–37.8	34.6–37.8	34.2–38
100 mA	33.6–38.2	33.4–38	33.2–37.8	34.8–38	35.2–38	34.6–38
200 mA	33.4–38.2	33–38	33–38	34.4–38.2	34.8–38	34.4–38
300 mA	33.2–38.2	32.8–38	32.8–38	34.2–38.4	34.6–38	34.2–38.2
500 mA	33–38.2	32.6–38	32.6–38	34–38.4	34.2–38.2	34–38.4

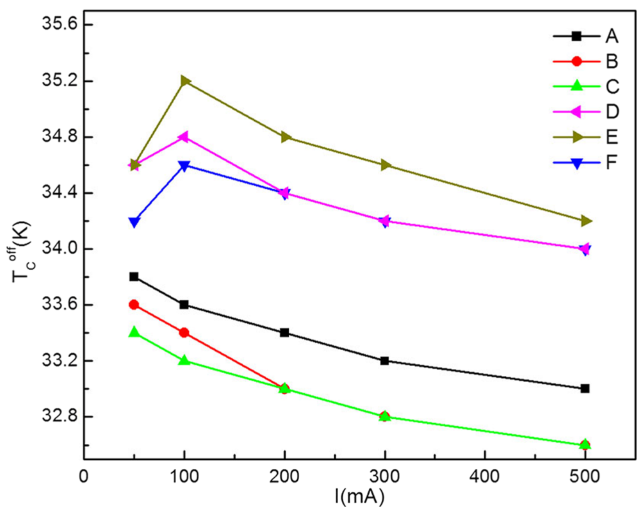

Fig. 7 The relationship between the T_C^{off} of doped samples and currents

unconventional superconductors ZrNCl and MoS_2. ZrNCl and MoS_2 show T_C of 15.2 and 10.8 K, respectively, on the optimum carrier doping [27, 28]. Nevertheless, in our experiment, the effect of changing electric field on the T_C is not obvious; this may be because we change the carrier density by changing the current directly rather than changing the electric field to induce carrier density change.

4 Conclusion

On the basis of the smart metamaterial superconductor model, we found that the inhomogeneous phase significantly improves the T_C of a superconductor. In this paper, the responses of the T_C of MgB_2 to inhomogeneous phase doping and changing the applied electric field are systematically investigated. At first, we prepared $Y_2O_3:Eu^{3+}$ and Y_2O_3, $Y_2O_3:Sm^{3+}$ nanosheet inhomogeneous phases, which were doped into MgB_2 by an ex situ process. Results showed that the T_C^{off} of MgB_2 doped with $Y_2O_3:Eu^{3+}$ nanosheets increase by 1.2 K compared with that of pure MgB_2, whereas the T_C^{off} of MgB_2 doped with Y_2O_3 and $Y_2O_3:Sm^{3+}$ nanosheets decrease, and the MgB_2 doped with $Y_2O_3:Sm^{3+}$ nanosheets presents the lowest T_C^{off}. In addition, the T_C^{on} of all of the MgB_2 doped with nanosheets decrease. The distribution of certain chemical elements reveals that $Y_2O_3:Eu^{3+}$ nanosheets inhomogeneous phase dopants distributed around the MgB_2 particles and formed a meta-structure. Hence, the effectiveness of $Y_2O_3:Eu^{3+}$ nanosheets which improves the T_C of MgB_2 can be fully reflected. Then, on the basis of the idea that changing the effective dielectric constant can increase the superconducting transition temperature of a meta-superconductor, we prepared MgB_2 doped with $Y_2O_3:Eu^{3+}$ microsheets and nano-Ag solution to change the dielectric constant of the system so as to improve the superconducting transition temperature of MgB_2. Nevertheless, experimental results show that the codoping cannot improve the T_C of MgB_2. Additionally, the superconducting transition temperature of MgB_2 doped with nano-Ag solution decreases remarkably, and the resistivity in the normal state increases. Finally, we also find that the applied electric field affects the T_C of doping samples; when increasing the test current, the T_C^{off} of nonluminous inhomogeneous phase doping samples decrease. However, the T_C^{off} of luminescent inhomogeneous phase doping samples increase and then decrease. The T_C^{on} of pure MgB_2 showed no change, whereas the T_C^{on} of doped samples can more than 38.2 K at certain conditions. Improving the superconducting transition temperature of MgB_2 can not only increase its application but also promote the development of superconductivity theory. This study provides a further exploration for the considerable challenge of improving the T_C of smart meta-superconductor MgB_2.

Acknowledgments This work was supported by the National Natural Science Foundation of China for Distinguished Young Scholar under Grant No. 50025207.

References

1. Nagamatsu, J., Nakagawa, N., Muranaka, T., Zenitani, Y., Akimitsu, J.: Nature **410**(6824), 63–64 (2001)
2. Yamashita, T., Buzea, C.: Supercond. Sci. Technol. **14**(11), R115–R146 (2001)
3. Slusky, J.S., Rogado, N., Regan, K.A., Hayward, M.A., Khalifah, P., He, T., Inumaru, K., Loureiro, S.M., Haas, M.K., Zandbergen, H.W., Cava, R.J.: Nature **410**(6826), 343–345 (2001)
4. Luo, H., Li, C.M., Luo, H.M., Ding, S.Y.: J. Appl. Phys. **91**(10), 7122 (2002)
5. Cava, R.J., Zandbergen, H.W., Inumaru, K.: Phys. C. **385**, 8–15 (2003)
6. Kazakov, S.M., Puzniak, R., Rogacki, K., Mironov, A.V., Zhigadlo, N.D., Jun, J., Soltmann, C., Batlogg, B., Karpinski, J.: Phys. Rev. B. **71**(2), 024533 (2005)
7. Bianconi, A., Busby, Y., Fratini, M., Palmisano, V., Simonelli, L., Filippi, M., Sanna, S., Congiu, F., Saccone, A., Giovannini, M., De Negri, S.: J. Supercond. Nov. Magn. **20**(7), 495–501 (2007)
8. Monni, M., Affronte, M., Bernini, C., Di Castro, D., Ferdeghini, C., Lavagnini, M., Manfrinetti, P., Orecchini, A., Palenzona, A., Petrillo, C., Postorino, P., Sacchetti, A., Sacchetti, F., Putti, M.: Physica C **460–462**, 598–599 (2007)
9. Zhao, Y.G., Zhang, X.P., Qiao, P.T., Zhang, H.T., Jia, S.L., Cao, B.S., Zhu, M.H., Han, Z.H., Wang, X.L., Gu, B.L.: Physica C **361**(2), 91–94 (2001)
10. Pendry, J.B., Holden, A.J., Stewart, W.J., Youngd, I.: Phys. Rev. Lett. **76**, 4773 (1996)
11. Pendry, J.B., Holden, A.J., Robbins, D.J., Stewart, W.J., Trans, I.: Microw. Theory Tech. **47**, 2075 (1999)
12. Shelby, R.A., Smith, D.R., Schultz, S.: Science **292**, 77 (2001)
13. Liu, H., Zhao, X.P., Yang, Y., Li, Q.W., Lv, J.: Adv. Mater. **20**(11), 2050–2054 (2008)
14. Qiao, Y.P., Zhao, X.P., Su, Y.Y.: J. Mater. Chem. **21**(2), 394–399 (2011)
15. Zhao, X.P.: J. Mater. Chem. **22**(19), 9439–9449 (2012)

16. Jiang, W.T., Xu, Z.L., Chen, Z., Zhao, X.P.: J. Funct. Mater. **38**, 157–160 (2007). in Chinese, available at http://www.cnki.com.cn/Article/CJFDTOTAL-GNCL200701046.htm
17. Xu, S.H., Zhou, Y.W., Zhao, X.P.: Mater. Rev. **21**, 162–166 (2007). in Chinese, available at http://www.cnki.com.cn/Article/CJFDTotal-CLDB2007S3048.htm
18. Zhang, Z.W., Tao, S., Chen, G.W., Zhao, X.P.: J. Supercond. Nov. Magn. **29**(5), 1159–1162 (2016)
19. Tao, S., Li, Y.B., Chen, G.W., Zhao, X.P.: J. Supercond. Nov. Magn. **30**, 1405–1411 (2016)
20. Smolyaninov, I.I., Smolyaninova, V.N.: Adv. Condens. Matter Phys. **2014**, 479635 (2014)
21. Smolyaninova, V.N., Yost, B., Zander, K., Osofsky, M.S., Kim, H., Saha, S., Greene, R.L., Smolyaninov, I.I.: Sci. Report. **4**, 7321 (2014)
22. Smolyaninova, V.N., Zander, K., Gresock, T., Jensen, C., Prestigiacomo, J.C., Osofsky, M.S., Smolyaninov, I.I.: Sci. Report. **5**, 15777 (2015)
23. Smolyaninov, I.I., Smolyaninova, V.N.: Phys. Rev. B. **91**, 094501 (2015)
24. Smolyaninova, V.N. et al.: Sci. Report. **6**, 34140 (2016)
25. Wang, S.S., Ning, X.S., J, M.S., Li, H., Chu, X.H.: Cryo. & Supercond. **40**(8), 1–6 (2012). in Chinese, available at http://www.cnki.com.cn/Article/CJFDTOTAL-DWYC201208002.htm
26. Li, J.S.: Physics Examination and Testing **28**, 3 (2010). in Chinese, available at http://www.cnki.com.cn/Article/CJFDTOTAL-WLCS201003006.htm
27. Ye, J.T., Inoue, S., Kobayashi, K., Kasahara, Y., Yuan, H.T., Shimotani, H., Iwasa, Y.: Nat. Mater. **9**, 125–128 (2010)
28. Ye, J.T., Zhang, Y.J., Akashi, R., Bahramy, M.S., Arita, R., Iwasa, Y.: Science **338**(6111), 1193–1196 (2012)
29. Chen, G.W., Li, Y.B., Qi, W.C., Yang, C.S., Zhao, X.P.: J. Mater. Sci.: Mater. Electron. (2017). https://doi.org/10.1007/s10854-017-8213-7
30. Qi, W.C., Chen, G.W., Yang, C.S., Luo, C.R., Zhao, X.P.: J. Mater. Sci.: Mater. Electron. **28**, 9237–9244 (2017)
31. Cai, Q., Liu, Y.C., Ma, Z.Q., Dong, Z.: J. Supercond. Nov. Magn. **25**, 357 (2012)
32. Igor, I.S., Vera, N.S.: Phys. Rev. B. **93**, 184510 (2016)